

Article - Health Science/Pharmacognosy

Liquid Crystals as a Vehicle for *Croton tiglium* L. Oil for Deep Chemical Peel Formulations

Anna Claudia Morais de Oliveira Capote¹

<https://orcid.org/0000-0003-2960-5428>

Patricia Mazureki Campos²

<https://orcid.org/0000-0003-2659-8023>

Cecília Cardozo Costa²

<https://orcid.org/0000-0002-6476-4646>

Nicole Ribas Modesto da Silva²

<https://orcid.org/0000-0002-5347-976x>

Priscileila Colerato Ferrari²

<https://orcid.org/0000-0002-4285-6646>

Marcelo Paulo Bueno da Silva⁴

<https://orcid.org/0000-0002-1998-0956>

Carla Cristine Kanunfre⁴

<https://orcid.org/0000-0002-2865-3084>

Francieli Kanunfre de Carvalho¹

<https://orcid.org/0000-0002-5336-257X>

Carlos Gustavo Wambier³

<https://orcid.org/0000-0002-4636-4489>

Evelyn Assis de Andrade¹

<https://orcid.org/0000-0002-7542-3070>

Wendy Karen Strangman⁵

<https://orcid.org/0000-0002-6911-4909>

Flávio Luís Beltrame^{1,2*}

<https://orcid.org/0000-0001-7067-5802>

¹Universidade Estadual de Ponta Grossa, Programa de Pós-Graduação em Ciências Farmacêuticas, Ponta Grossa, Paraná, Brasil; ²Universidade Estadual de Ponta Grossa, Departamento de Ciências Farmacêuticas, Ponta Grossa, Paraná, Brasil; ³The Warren Alpert Medical School of Brown University, Department of Dermatology, Rhode Island, USA; ⁴Universidade Estadual de Ponta Grossa, Departamento de Biologia Geral, Ponta Grossa, Paraná, Brasil; ⁵University of North Carolina Wilmington, Department of Chemistry and Biochemistry, Wilmington, North Carolina, USA.

Editor-in-Chief: Paulo Vitor Farago
Associate Editor: Jane Manfron Budel

Received: 20-Jan-2023; Accepted: 20-Jul-2023

*Correspondence: flaviobeltra@gmail.com; Tel.: +55(42)99960-1108 (F.L.B.)

HIGHLIGHTS

- *Croton tiglium* oil is a peel's active component.
- Phorbol esters are present in this vegetal matrix.
- Liquid crystals can encapsulate the active compounds of *Croton tiglium* oil.
- Lamellar liquid crystalline phase at nanometric size, narrow PDI and negative zeta potential.
- Liquid crystals loaded with croton oil showed suitable stability over 28 days.

Abstract: Historically, phenol/croton oil deep chemical peeling has been very effective and has generated excellent results compared to other formulas used in dermatological clinics. However, it can cause serious side effects in patients sensitive to phenol. Therefore, this study aimed to develop a liquid crystalline structure containing croton oil (without phenol) as well as to evaluate the physical characteristics and cytotoxicity of this new system. Rational proportions of the croton oil, purified water, and polyethylene glycol hexadecyl ether were designed through a partial phase diagram to obtain 26 formulations. After macroscopic analysis and polarized light microscopy evaluation, formulations with lamellar liquid crystalline phase (4 samples) were identified and chosen to determine pH, size, polydispersion index (PDI), zeta potential, and rheological behavior. After 48 hours, three samples presented phase separation. Formulation 8 remained stable, but hydroxyethyl cellulose (HEC, 0.5%, w/w) was added to the aqueous phase, to prevent coalescence. Sample 8A exhibited a pH compatible with the skin, nanometric size, narrow PDI, negative zeta potential, and stability throughout the study period. The addition of HEC improved the organization of the system, making the formulation more stable. The oil, fractions of the oil, and the sample exhibited increasing cytotoxicity, respectively. This result could be attributed to the fractionation process of the vegetal matrix, and the surfactant present in the formulation increased the cell membrane permeability. The proposed approach successfully achieved a physically stable liquid crystal system containing croton oil.

Keywords: chemical peels; phenol; liquid crystals; Drug Delivery System (DDS); topical application.

INTRODUCTION

Chemical peeling involves the controlled wounding of the epidermis and dermis for both medical and aesthetic improvement [1].

Hetter formulas are an example of formulations that promote deep peeling, which contains phenol 88% (w/v), croton oil, liquid soap (Septisol®), and purified water as components [2]. This mixture can form a suspension that requires shaking prior to topical application to achieve homogeneity, due to the instability of liquid soap containing formulations. It is still used in clinical practices, even though the cotton-tipped applicator (swab) can add heterogeneous amounts of ingredients on the skin [3].

The *Croton tiglium* oil (CO, obtained from the *Crotonis fructus*) is considered the active component of the peel formulation. It contains terpenes (especially diterpenes – phorbol esters) [4] which exhibit pro-inflammatory properties [5]. These phorbol esters are responsible for stimulating the secretion of cytokines by several inflammatory cells in the dermis [3]. Phenol, being highly lipophilic, serves as a vehicle for CO, aiding in the permeation of phorbol esters present in the vegetal matrix. Additionally, it is known that phenol can promote the coagulation of upper dermis capillaries, reducing the phorbol esters systemic absorption [3,6]. However, there are undesirable effects coming from phenol due to its high toxicity and high risk of causing complications, such as cardiac effects, liver diseases, and nephrotoxicity. Although the use of Hetter formulas and knowledge regarding phenol toxicity have been well-established, physicians should be aware of these aspects.

Based on the above, alternatives need to be explored to reduce the toxicity of this formula while maintaining the desired effectiveness of the active component (responsible for the peeling effect) into an adequate vehicle. One promising system for transporting and releasing the active compounds of CO into the deep skin layers is liquid crystals (LC). The LC represents a third phase of the nanostructures, which can be used in cosmetic and pharmaceutical formulations. They can encapsulate the active substances and ensure the delivery at a controlled release propitiating high concentration at the interest site through skin permeation with systems of increased stability [7]. An effective LC platform may be composed of water and amphiphilic lipids, such as the nonionic surfactant (polyethylene glycol hexadecyl ether/polyoxyethylene-20 cetyl ether); it had been extensively explored in basic formulation development with a mixture of this compound and glycerol, showing the micellization and salting-out effects of the surfactant [8]; mixture with temperature sensitive-hydrogel [9]; its association with polyoxyethylene-20 sorbitan monooleate and polyoxyethylene-4 lauryl ether in a ternary diagram study [10], and its combination with oleic acid, N-methylpyrrolidone, and isopropyl myristate for carrying dexamethasone in an innovative formulation [11]. This lyotropic carrier can maintain the liquid crystalline structure in the emulsion's internal phase, providing physicochemical protection to the encapsulated substance [12].

They are notable for their ability to self-organize symmetrically in two- and three-dimensional systems, containing hydro and lipophilic molecules of different sizes. Most of these LC systems are modulated to exhibit different phases to be applied for various purposes, including drug delivery and vaccine platforms, by manipulating their internal structures to acquire different conformations and properties to be administered through several routes [13,14]. LC systems can disrupt biological barriers and overcome, for example, the

skin and mucosa, due to enhanced retention and permeation effects. This mechanism involves temporary disorganization of these barriers, with the creation of holes through which the encapsulated substances can penetrate freely into deeper layers [14].

Based on these considerations, this study proposes the development of an LC system loaded with CO, as well as their microscopic, macroscopic, rheological, physical evaluation, and cytotoxic qualification, aiming future pre-clinical and clinical studies to evaluate this formulation as a new product to be used in peeling procedures.

MATERIAL AND METHODS

Materials

CO was purchased from Delasco[®] (United States of America), purified water was produced by MilliQ[®] system (Germany), polyethylene glycol hexadecyl ether was supplied from Sigma-Aldrich[®] (United States of America), and hydroxyethyl cellulose was purchased from Delaware[®] (Brazil). Murine fibroblast cells (3T3, code No. 0017, CRL-1658) were obtained from the American Type Culture Collection (ATCC, Brazil), RPMI[®] 1640 medium and fetal bovine serum were purchased from Vitrocell[®] (Brazil); 3-(4,5-dimethylthiazol-2-yl)-2,5-diphenyltetrazolium bromide (MTT), sodium bicarbonate, glutamine, sodium pyruvate, dimethylsulfoxide (DMSO), 96 well plates, penicillin, and streptomycin were purchased from Sigma–Aldrich-MERCK[®] (Brazil).

Methods

Preparation of CO fractions and CO UPLC-MS/MS analyses

The CO (30 mL) was adsorbed on silica and placed in a Soxhlet apparatus. Subsequently, it was extracted for 5 hours with 200 mL of each solvent (petroleum ether, hexane, dichloromethane, ethyl acetate, methanol, and aqueous, added subsequently). The solvents were evaporated under vacuum at 40 °C and lyophilized; the dried samples were stored under refrigeration (5 °C) until the moment of use. UPLC-MS/MS analyses of the methanol fractions (1%, v/v) were carried out on a Waters[®] I-Class UPLC coupled to a Waters[®] G2-XS Quadrupole Time of Flight (Q-TOF) Mass Spectrometer. The separation was carried out on a Acquity UPLC[®] BEH C18 1.7 µm, 2.1 x 100 mm reversed-phase column with 0.1 % formic acid in water (v/v) (solvent A) and 0.01% formic acid in acetonitrile (v/v) (solvent B). The temperature of the column was 30 °C. A volume of 3 µL was injected with a flow rate of 0.45 mL/min. The separation was achieved with a run time of 10 minutes through positive and negative ESI mode by following the gradient method (5% of solvent B until 7.0 minutes; increase to 100% of solvent B until 8.5 minutes; returning to 5% of solvent B until 10 minutes). The ion range was between 50-1800 mass to charge ratio (m/z). Additionally, UPLC-MS/MS acquisition was also performed in the positive mode with a fixed collision energy of 20 eV and a fixed m/z 311.16, and the acquisition time ranged from 4.5 to 7.0 minutes.

Preparation of the LC formulations

The experimental formulations were prepared using different amounts of the surfactant (polyethylene glycol hexadecyl ether - S), CO (oily phase – OP), and purified water (aqueous phase – AP). Briefly, the amounts of the components (2 grams for each formulation) were individually heated at 40 °C and weighed according to a partial ternary phase diagram. The surfactant was added to the OP and after mixture, the AP was added. The preparation was stirred for 3 minutes using vortex-mixing. Finally, the emulsions were stored away from heat and light for 24 hours for equilibration before analysis. The samples were stored at room temperature (between 17 - 20 °C), protected from light. The chemical composition of the formulations is presented in Table 1.

Table 1. Chemical composition of formulations obtained from the partial ternary phase diagram construction.

% components (w/w)/ Formulations	Polyethylene glycol hexadecyl ether (Surfactant)		Croton oil (Oily Phase – OP)		Purified water (Aqueous Phase – AP)	
	%	grams	%	grams	%	grams
1	10	0.2	80	1.6	10	0.2
2	10	0.2	70	1.4	20	0.4
3	10	0.2	60	1.2	30	0.6
4	10	0.2	50	1.0	40	0.8
5	10	0.2	40	0.8	50	1.0
6	10	0.2	30	0.6	60	1.2
7	10	0.2	20	0.4	70	1.4
8	10	0.2	10	0.2	80	1.6
9	20	0.4	70	1.4	10	0.2
10	20	0.4	60	1.2	20	0.4
11	20	0.4	50	1.0	30	0.6
12	20	0.4	40	0.8	40	0.8
13	20	0.4	30	0.6	50	1.0
14	20	0.4	20	0.4	60	1.2
15	20	0.4	10	0.2	70	1.4
16	30	0.6	60	1.2	10	0.2
17	30	0.6	50	1.0	20	0.4
18	30	0.6	40	0.8	30	0.6
19	30	0.6	30	0.6	40	0.8
20	30	0.6	20	0.4	50	1.0
21	30	0.6	10	0.2	60	1.2
22	40	0.8	50	1.0	10	0.2
23	40	0.8	40	0.8	20	0.4
24	40	0.8	30	0.6	30	0.6
25	40	0.8	20	0.4	40	0.8
26	40	0.8	10	0.2	50	1.0

After initial physical analyses, sample 8 was chosen and hydroxyethyl cellulose (0.5 %, w/w) was added into the AP. The homogenization process was extended to 6 minutes in a vortex-mixer.

Macroscopy characterization

The formulations were examined to verify homogeneity and appearance. The parameters were determined as phase separation, and color observation (opaque, clear, milk, or oily), respectively. Samples without phase separation were chosen, and all analyses were performed in duplicate.

Microscopy evaluation

The formulations were evaluated through a polarized light microscope equipped with a BX 5 camera (Olympus®, Japan) to identify the liquid crystalline phase. The analyses were executed at magnifications of 50x and 200x. All analyses were performed in duplicate.

Physical characterization

Physical analyses of the formulations containing the LC were measured using dynamic light scattering (DLS) by intensity for average particle size, polydispersity index (PDI), electrophoretic mobility for zeta potential with a Zetasizer Nano ZS® instrument (Malvern Instruments®, United Kingdom). The measurements were performed with formulations diluted in purified water (1:10, v/v) at 25 °C with a He-Ne laser operating at a scattering angle of 90 °. The zeta potential was determined in the equipment cuvette (DTS 1070) at 25 °C. The pH measurements were carried out using a digital potentiometer MB-10 (Marte®, Brazil) previously calibrated with pH 4.0 and 7.0 buffer solutions. Prior to measurements, the samples/formulations were diluted in purified water (1:10, v/v) at 25 °C, and mixed for 10 seconds in a vortex-mixer. All analyses were performed in duplicate.

Rheological evaluation

Rheological measurements were conducted using an oscillatory mode rheometer (DHR-2/ TA Instruments, Germany) at 25 °C, with a parallel cone-plate geometry of 40 mm diameter, separated by a fixed distance of 0.057 mm. The samples (1 g) were carefully applied to the bottom plate of the rheometer, ensuring minimal shear of the formulation and allowing a rest time (relaxation of the introduced tension before analysis) of 1 minute before each determination. The amplitude was 1%, and a frequency range of 0.01 to 100 Hz was analyzed for each sample. The elastic modulus (G'), viscous modulus (G''), and complex viscosity (η^*) were determined. All analyses were performed in duplicate.

Physical stability

Macroscopy and microscopy evaluations were executed as well as pH, size, PDI, zeta potential determinations, and rheological studies (n= 2) at times of 0, 1, 7, 14, 21 and 28 days.

Encapsulation efficiency (EE) of CO

The content of terpenes in the formulation was determined according to the method described by Fan and He [15], with some adaptations. Briefly, 600 μ L of the emulsion with LC was filtered (Amicon[®] ultra-centrifugal filter devices, Millipore[®], Germany) with a molecular weight cut-off of 50 kDa, after centrifugation in Hermle (model z326k, Germany) in 3885 g for 30 minutes at 4 °C. The supernatant (free drug into de ultrafiltrate – M_{FD}), and 100 μ L of the formulation (total drug amount – M_{TD}) were collected and mixed, respectively, with 150 μ L of vanillin solution in glacial acetic acid (5 %, w/v) and 500 μ L of perchloric acid. The samples were then heated for 60 minutes at 60 °C and cooled in an ice water bath at room temperature. The content of terpenes was measured at 548 nm using a plate reader (μ Quant Biotek[®], United States of America). To calculate the EE, the formula $EE (\%) = [(M_{TD} - M_{FD}) / M_{TD}] \times 100$ was used. To determine the amount of terpenes in the sample, 0.2 g of CO was weighted, and serial dilutions were prepared and measured. In addition, a calibration curve of PMA (phorbol 12-myristate 13-acetate, Sigma-Aldrich[®], Germany) was performed by accurately weighting of 2 mg of the PMA and dissolving it in ethanol using a volumetric flask (25 mL). Dilutions were performed to obtain solutions with a concentration range between 56 to 80 μ g/mL. The calibration standards were prepared in triplicate, and the calibration curve was drawn by plotting the absorbance against the compound concentration ($y=0.0019x + 0.1376$, $r = 0.9902$). The results were expressed in mg of PMA per g of croton oil/sample.

Cell Culture

Non-neoplastic adherent cell 3T3 was maintained in RPMI[®] 1640 medium (pH 7.4) supplemented with 10 % fetal bovine serum (FBS), 24 mM of sodium bicarbonate, 2 mM of glutamine, 1 mM of sodium pyruvate, 10,000 U of penicillin, and 10 mg of streptomycin per liter of medium (under controlled temperature and humidified atmosphere – 37 °C and 5 % CO₂, respectively). The same conditions were applied to cell and subcultures expansions. For the cells used in this study, no more than 30 cell passages were applied, and the cultures did not exceed 3 months.

Cell viability - MTT reduction assay

The assay was executed according to the standardized method described by Cruz and coauthors [16]. In brief, adherent cells in the logarithmic growth phase were seeded in 96-well plates (3x10³ cell/well), different concentrations of CO (250-1500 μ g/mL) and CO fractions (100-1200 μ g/mL), solubilized in DMSO (final concentration: < 0.25 %), were added to the cells and incubated for 72 hours. The cells were also treated with the LC formulation (0.01-100 μ g/mL) solubilized in the culture medium. After the treatment period, the culture medium was removed, and 200 μ L of MTT solution (0.5 mg/mL) was added to each well. The plates were then incubated at 37 °C for 2 hours. Following the incubation, the formazan crystals formed were solubilized in DMSO and the optical density was measured at 550 nm using a plate reader (μ Quant Biotek[®], United States of America). The negative control (non-treated cells) was prepared in the same way as described above, but the cells were incubated with 0.25 % DMSO in RPMI medium or the surfactant (polyethylene glycol hexadecyl ether), to the LC formulation. All tests were performed in triplicate. The percentage of growth inhibition was determined based on the formula:

$$\% \text{ of growth} = (\text{Optical density of treated cells} / \text{Optical density of negative control}) \times 100$$

Statistical analysis

Data were expressed as mean \pm standard deviation (SD). The cell viability results were assessed using one-way analysis of variance (ANOVA) followed by Tukey's post-test. A significance level of 5% ($\alpha = 0.05$) was considered to determine statistical significance. The cell viability and stability data were analyzed using the GraphPad Prism[®] software (GraphPad Software Inc., version 6.01 for Windows[®]). The cytotoxic results were expressed as IC₅₀, which was calculated using Probit analysis with Finney's method (StatPlus Software, version 5). For the physical analyses, statistical comparisons were conducted using Tukey's post-test, with a significance level of 5 % ($\alpha = 0.05$). Rheological data were obtained from Trios[®] 5.2 software (TA Instruments), and the curves describing the characteristics of the formulations were plotted using OriginPro[®] 9.0 software.

RESULTS

Preparation of the LC formulations and macro- and microscopy characterization

The formulations were prepared based on the ternary partial phase diagram (Figure 1).

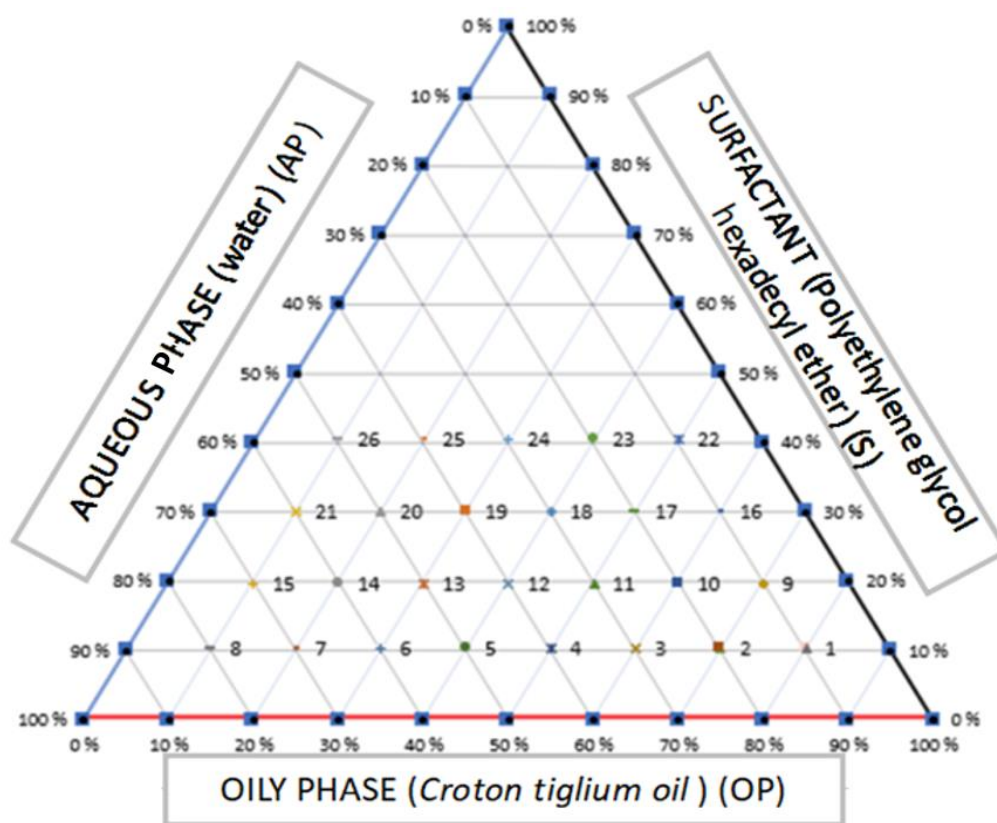


Figure 1. Partial phase diagram proposal.

All 26 samples showed a homogeneous and creamy appearance, but they varied in terms of turbidity, with 14 opaque samples and 12 milky samples (data not shown). These samples were evaluated by polarized light microscopy and according to the liquid crystalline structure observed, the systems were characterized, and samples that formed a lamellar phase were selected, being 9 of 26 samples. Five formulations were excluded from further analysis due to their similar chemical composition, CO concentration, and low amount of lamellar phase, when compared to the selected formulations. Formulations numbered 1, 3, 5, and 8 (Figure 2) were selected and the Maltese cross formation was confirmed, a characteristic pattern for this type of LC system called lamellar phase.

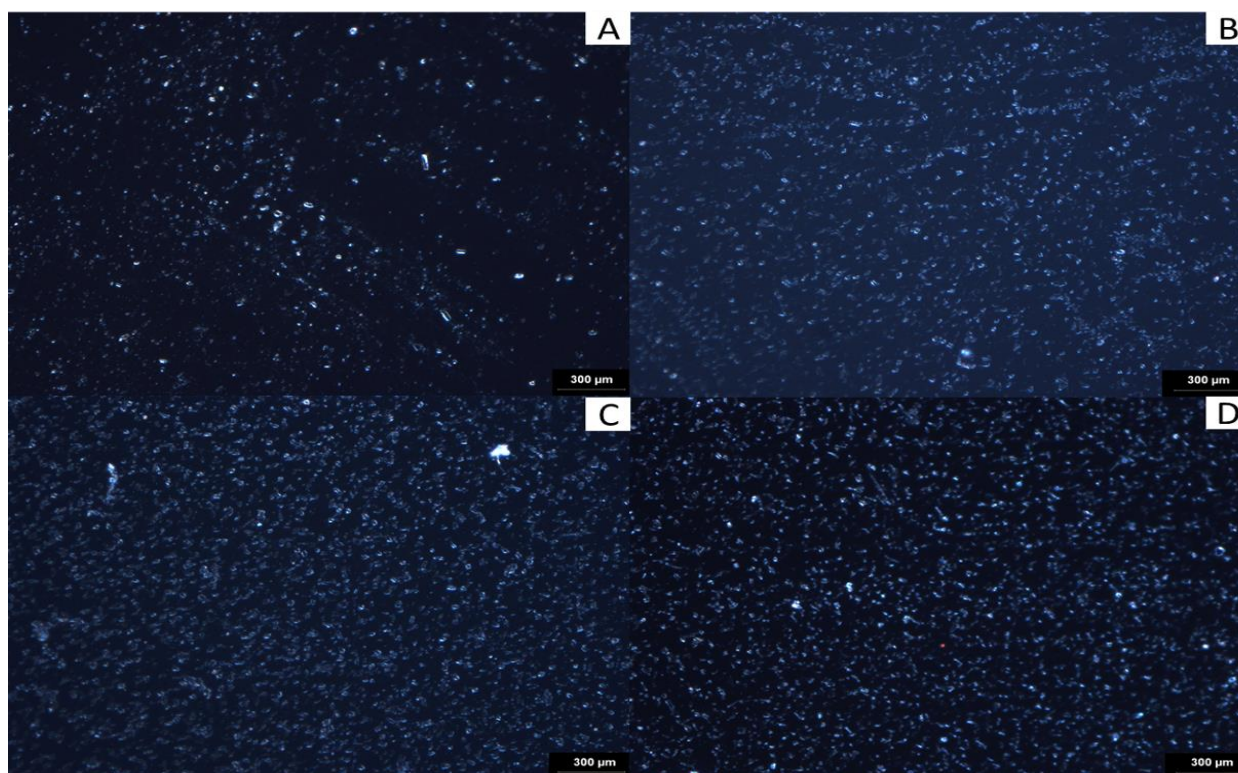


Figure 2. Characterization by polarized light microscopy of the formulations containing lamellar liquid crystalline phases: A) formulation 1 (S10%/OP80%/AP10%, w/w/w); B) formulation 3 (S10%/OP60%/AP30%, w/w/w); C) formulation 5 (S10%/OP40%/AP50%, w/w/w); D) formulation 8 (S10%/OP10%/AP80%, w/w/w). The image was observed at magnification of 50x.

Physical characterization

Table 2 shows the physical results of the formulations. The pH values were around 6.0. The zeta potential values obtained for all formulations analyzed ranged from -15.1 to -27.5 . The mean particle size ranged from 225 to 521 nm. Samples 1 and 8 exhibited a homogeneous distribution, as indicated by low PDI values. However, samples 3 and 5 showed heterogeneous particle sizes.

Table 2. Physical parameters for the formulations developed.

Formulation/ Physical parameters	1 (S10%/OP80%/AP10%, w/w/w)	3 (S10%/OP60%/AP30%, w/w/w)	5 (S10%/OP40%/AP50%, w/w/w)	8 (S10%/OP10%/AP80%, w/w/w)
pH	6.05 ± 0.010	6.425 ± 0.005	6.50 ± 0.005	6.71 ± 0.001
Zeta Potential (mV)	-27.58 ± 0.035	-15.1 ± 0.070	-21.85 ± 0.150	-23.85 ± 0.050
Polydispersion Index (PDI)	0.354 ± 0.004	1.000 ± 0.001	1.000 ± 0.002	0.161 ± 0.005
Particle size (nm)	423.85 ± 0.950	225.8 ± 1.100	521.45 ± 1.350	407.25 ± 0.600

Physical stability

After 48 hours, formulations 1, 3, and 5 showed phase separation, indicating instability. However, formulation 8 remained stable during this period, despite having similar physical parameters to the other formulations. To increase the physical stability and avoid coalescence, hydroxyethyl cellulose (0.5%, w/w) was added into the aqueous phase of formulation 8 (Table 3).

Table 3. Physical parameters for formulation 8A during the studied period.

Analysis day/ Test	Macroscopic Characteristic	pH	Zeta Potential (mV)	Polydispersion Index (PDI)	Particle size (nm)
0	Homogeneous Creamy (milky)	5.767± 0.621	-38.25± 0.869	0.565 ± 0.058	470.67 ± 78.748
1	Homogeneous Creamy (milky)	5.365 ± 0.173	-38.97± 2.041	0.536 ± 0.075	522.45 ± 55.486
8	Homogeneous Creamy (milky)	5.512± 0.009	-39.45± 3.239	0.453 ± 0.341	470.35 ± 135.509
14	Homogeneous Creamy (milky)	5.287± 0.015	-39.4± 5.428	0.346 ± 0.102	385.42 ± 39.756
21	Homogeneous Creamy (milky)	4.350± 0.212	-44.05± 0.070	0.516 ± 0.038	455.45 ± 0.141
28	Homogeneous Creamy (milky)	4.175± 0.007	-44.00± 0.001	0.583 ± 0.072	546.45 ± 2.050

The modified formulation (referred to as 8A) demonstrated stable behavior at room temperature for 28 days, with the persistence of a particle size around 500 nm, a polydispersity index less than 0.6, a negative zeta potential, and a pH close to the pH of the skin, although slightly decreased (Figure 3).

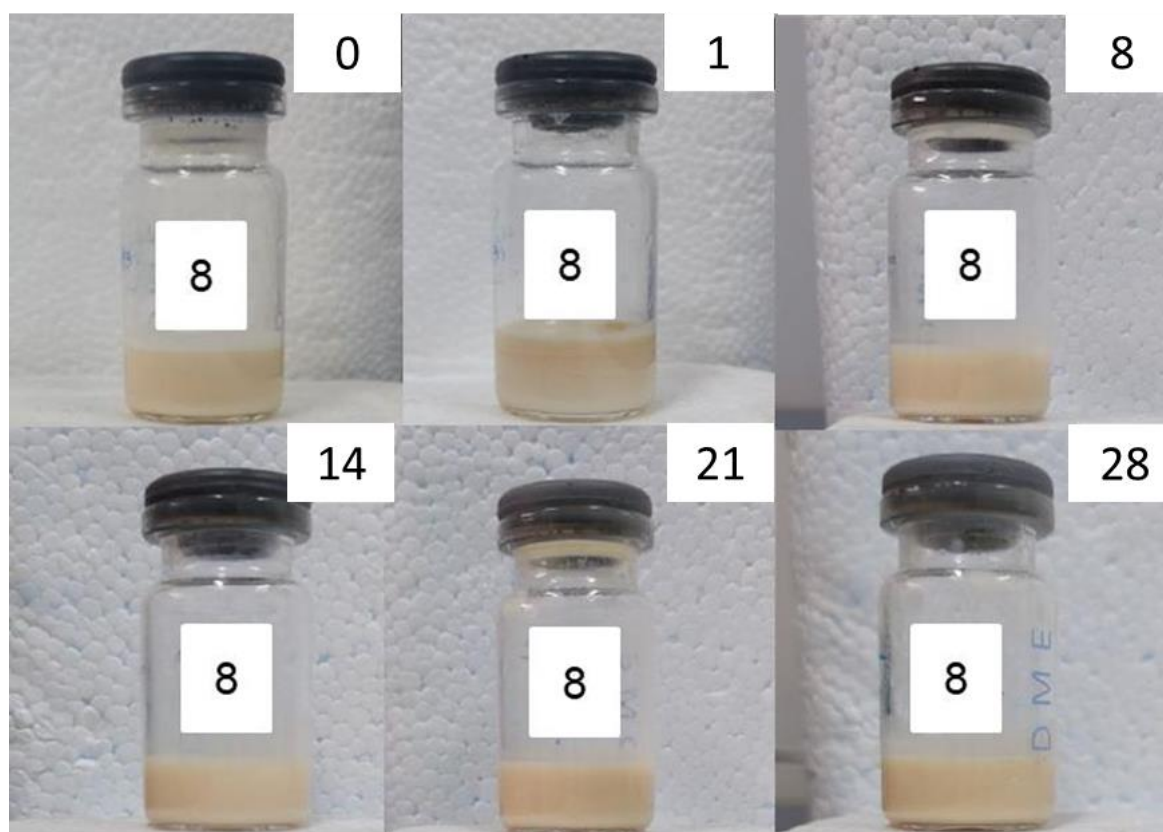


Figure 3. Macroscopic characteristics of formulation 8A (T10:O10:A80, w/w), with hydroxyethylcellulose in days 0, 1, 8, 14, 21 e 28.

Rheological evaluation

The viscoelastic properties of the LC formulations, such as the storage modulus G' and loss modulus G'' , were evaluated by varying the frequency, and the results are presented in Figure 4. For both samples,

storage modulus G' was parallel to loss modulus G'' , corresponding to lamellar phase behavior [17]. Formulation 8, without HEC, showed frequency-dependent behavior and a liquid-like viscosity; $G' < G''$ (Figure 4A, blue squares). The relation $G' > G''$ held for the HEC addition (sample 8A, black squares) across the frequency range tested, indicating a gel-like behavior [18]. Similarly, the complex viscosity was higher in formulation 8A, indicating an improved organization of the system and enhanced stability. Figure 4B shows the rheological behavior of formulation 8A after 1 and 28 days of preparation. Both time points exhibited similar behavior, indicating that the LC structure was maintained during the storage.

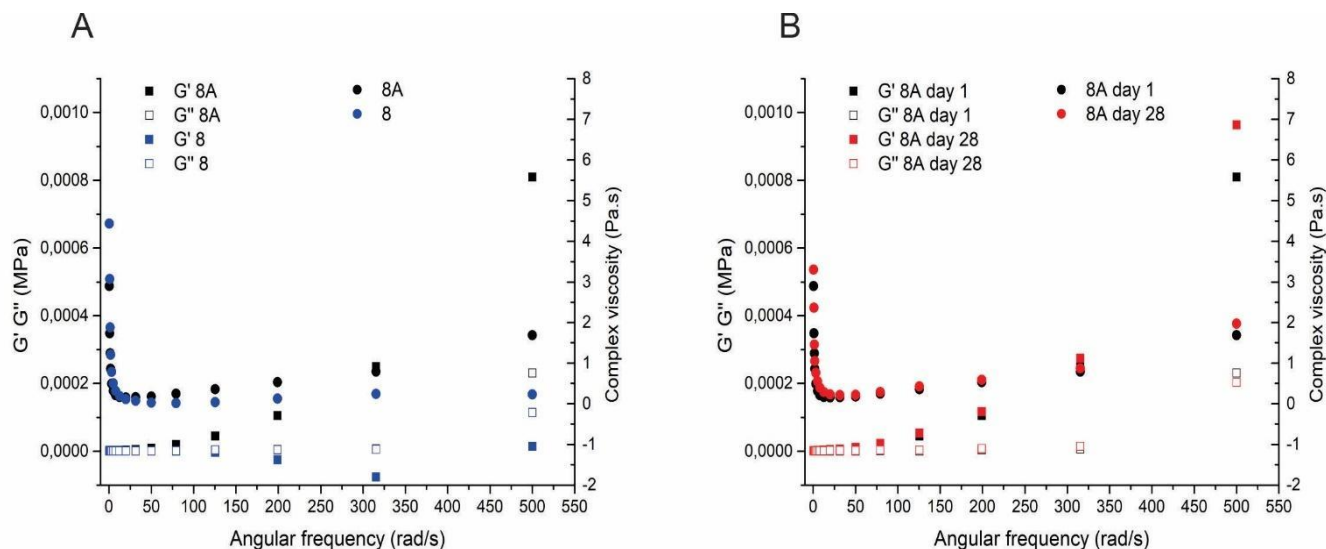


Figure 4. G' (filled squares), G'' (open squares), and complex viscosity (circles) as a function of the angular frequency of formulations (A) samples 8 and 8A, and (b) sample 8A day 1 and after 28 days of preparing, at $T = 25\text{ }^{\circ}\text{C}$.

Encapsulation efficiency (EE) and UPLC-MS/MS of CO

The quantification of terpenes in both the aqueous and oily phases confirmed the successful loading/incorporation of CO into the system (Table 4). The results revealed a high encapsulation efficiency of the formulation containing the lamellar liquid crystalline, near 100%, as well as high loading capacity ($\approx 50\%$), which considers the amount of drug encapsulated within the emulsion relative to the total amount of the internal phase.

Table 4. Results obtained for the quantification of total terpenes expressed in PMA in vegetal matrix (croton oil), and LC 8A sample (supernatant and filtrate).

Sample	μg of terpenes expressed in PMA per 200 mg of croton oil/sample
Croton oil	$1,316.40 \pm 32.52$
LC 8A (supernatant)	$1,218.13 \pm 77.56$
LC 8A (filtrate)	ND

Data are expressed as mean \pm standard deviation for three replicates. ND: not detected

The UPLC-MS/MS analysis of CO methanol fraction suggested the presence of phorbol structures in the formulation (Figure 5A). The UPLC-MS/MS data enabled the observation of phorbol esters presenting the diagnostic m/z 311 as a precursor (Figure 5B), with the transition m/z 311 \rightarrow 293 (Figure 5C and 5D).

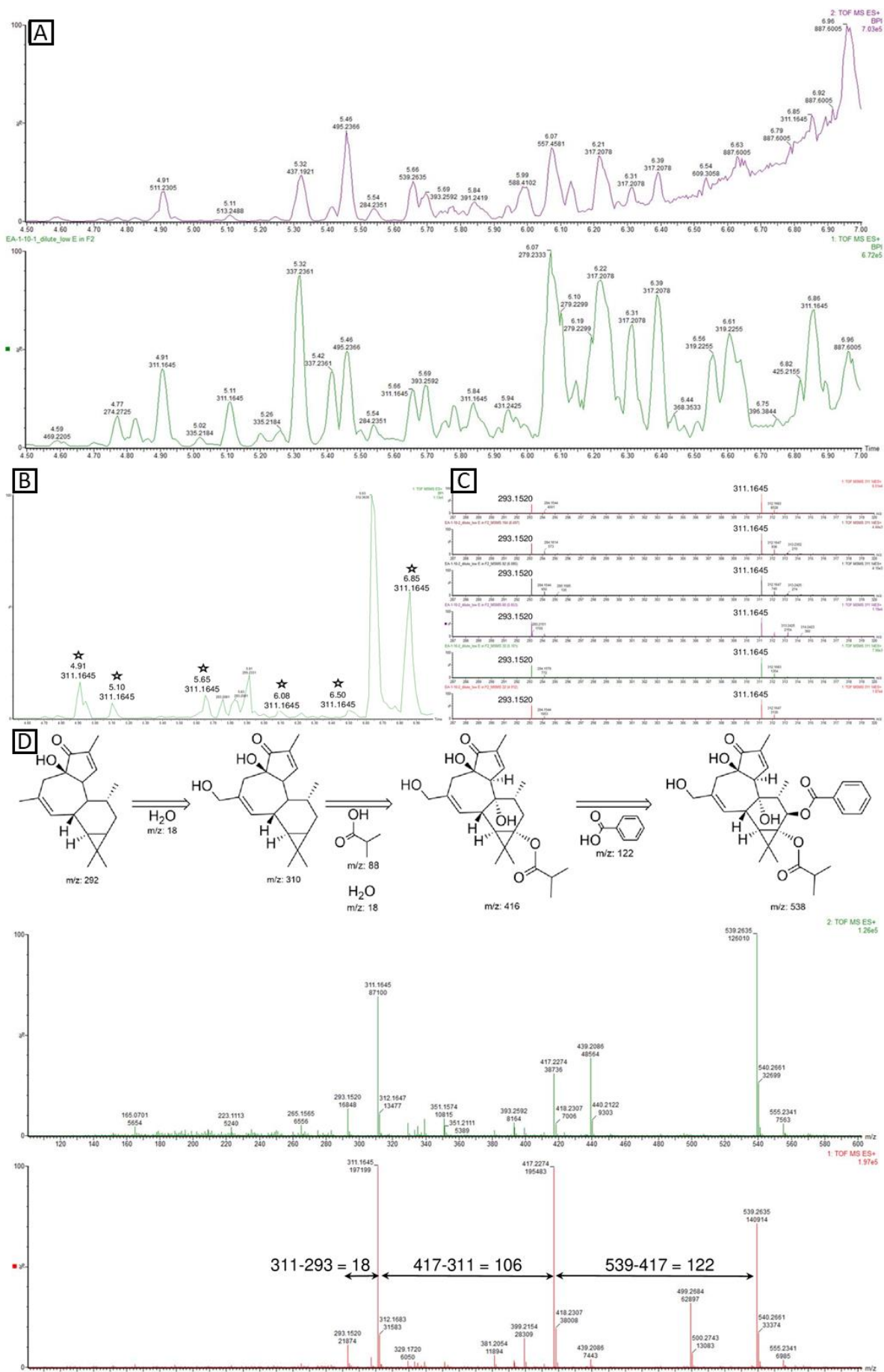


Figure 5. (A) Base peak intensity (BPI) chromatogram of CO MeOH fraction; (B) Fragmentation behavior of phorbol esters between 4.5 and 7.0 min; (C) UPLC-MS/MS of m/z 311; (D) MS-MS spectra of m/z 539.26 and proposed fragmentation patterns.

Cell viability study

The 72 hours evaluation of cellular treatment with CO and its fractions confirmed low cytotoxicity against 3T3 cells. The dichloromethane fraction exhibited higher toxicity compared to the other fractions and the crude oil itself. The LC sample (sample 8A) showed a higher cytotoxic effect compared to the CO and its fractions (Table 5).

Table 5. IC₅₀ values (µg/mL) for the treatment with croton oil, fraction of the vegetal matrix, and LC (formulation 8A) against normal cells (3T3) after 72 hours of treatment.

Sample	MTT reduction assay
	IC ₅₀ (µg/mL)
Pure oil	983.10 ± 37.85
Ether	>1200
Hexane	707.13 ± 26.61
Dichloromethane	308.70 ± 34.82
Methanol	898.81 ± 38.09
Aqueous	>1200
Sample 8A	2.92 ± 0.55
Polyethylene glycol hexadecyl ether	4.12 ± 0.80

DISCUSSION

This study was designed to propose the development of an LC system for the delivery of CO to be used as a new formulation for deep chemical peels, replacing the extemporaneous formulations used in dermatological clinics. It is because LC systems have the potential to protect loaded substances from degradation and have been shown to effectively deliver various active compounds through the stratum corneum [12,14].

Initially, a total of twenty-six (26) formulations were prepared and evaluated based on their macroscopic characteristics. It was observed that all formulations presented a creamy and homogeneous appearance, indicating the formation of a nanometric system [19]. However, it was also determined that according to the proportion of the components, different levels of the organization could be obtained, resulting in formulations with opaque, milky, or translucent characteristics [20]. It was found that a liquid crystalline phase could be achieved when the surfactant concentration was below 30% and the water content was high (above 80%), regardless of the CO concentration.

The polarized light microscopy technique is often applied to characterize the liquid crystalline structures in lipid-water systems due to its accessibility and ease of execution [21-22]. In this study, it was used to characterize the single-crystal quality and screen the phase properties of the LC system. It allowed for the observation of the birefringence and anisotropic textures, which are indicative of lamellar crystalline phases [21]. This phase is characterized by its lower viscosity compared to other mesophases and, usually, the formation of parallels double-chained of amphiphiles, known as the maltose cross pattern, which can be observed at higher magnifications [21-22]. The arrangement of the lipid tails of the amphiphiles may align with the triglycerides present in the CO, minimizing the entropy and facilitating the self-organization into a lamellar structure. Related to intermolecular forces, the polar head group's hydrogen bonds can interact strongly in comparison with the Van der Waals interaction between the hydrocarbon chains, where the lipid chains of CO can involve them [14,23]. Similar phase behavior was reported and confirmed by rheological studies that performed viscoelastic regions by the interaction of liquid-crystalline domains in the high-water contents [11].

The four (4) formulations selected presented a lamellar structure. For dermatological applications, this type of system is desirable as it contributes to prevent trans-epidermal water loss (TEWL) from the skin and maintains its flexibility and softness [24]. The potential of lamellar LC systems has been previously explored incorporated into the black *Dimocarpus longan* Lour. seeds extracts, demonstrating no irritancy and good stability, resulting in a cosmeceutical formulation for anti-wrinkle of the skin in anti-aging products [25]. The lamellar LC systems are preferred in cosmetic and dermatological applications due to their ability to solubilize hydro and lipophilic compounds. They also provide a less rigid texture compared to other types of liquid crystalline phases [14].

The pH of the selected formulations was around 5.5, which is considered suitable for dermatological application without causing damage to the skin. However, for a peeling preparation, lower pH values are desired as they can facilitate absorption and enhance the aggressiveness towards the epidermis [26]. Regarding the particle sizes, the four formulations were in the nanometric range (around 450 nm), which could be considered adequate for the skin application with enhanced permeation. Particle sizes between the range of 70-600 nm have been reported to accumulate in the epidermal and dermal layers, with a preference for aggregation in cutaneous appendages, thereby facilitating penetration into deep layers [12]. Although the formulations showed high PDI values, for formulation 8 the PDI represented a monodisperse population (around 0.16). The negative zeta potential values observed for all the formulations contribute to their electrical stability, particularly in the case of formulation 8. Nonetheless, Nekkanti and coauthors [27] reported that low electrostatic repulsive forces could potentially contribute to phase separation because the emulsion droplets electrostatic forces contribute to the systems stability. Moreover, non-optimal PDI values can contribute to the coalescence (droplets binding) of the systems and result in a loss of stability [28]. This indicates that further improvements can be made in the production process, such as optimizing homogenization conditions, temperature, speed, pressure, and other [14].

Overall, formulation 8 demonstrated the most favorable physical profile for a nano-dispersed system. It was also selected due to its lower CO concentration (10%, w/w) in comparison to the other formulations. The CO 10% (w/w) is suitable for skincare treatment at home, based on the skin anti-aging effects, such as the decrease of signs as wrinkles and hyperpigmentation, as reported in literature [29-30]. Further, this proposal of croton oil vehiculation in a formulation based-on liquid crystalline structure may propitiate the same benefits of those reached in dermatological clinical trials. After the incorporation of the hydrophilic polymer, the formulation 8A presented a PDI close to 0.5. The main finding was the maintenance of its PDI over 28 days, as indicated by the similar particle size distribution observed throughout this period. The colloidal stability of the system is aimed over time for topical application of liquid crystalline based-formulation and may be improved by the polymer addition as stabilizer to prevent particle aggregation and preserves the internal structure of the particles [31-32].

The rheological study, specifically the oscillatory rheological analysis, provides insights into the viscoelastic properties of the formulations, which are indicative of the structural nature of the system, directly implying the formulation's performance. The G' represents the energy stored during deformation when the stress increases and the energy released when the tension is relaxed. The G'' is the viscous element that cannot store energy because the applied stress dissipates through irreversible deformation. The addition of HEC in the formulation resulted in an increase in the mean values of the storage modulus G' , suggesting more structural organization. Similar findings have been reported in other oscillatory rheological studies conducted on LC systems. The hexagonal and lamellar crystalline mesophases generally have a G' greater than G'' , which reflects their high degree of structural organization [33].

The developed LC formulation 8A has demonstrated the ability to maintain the physical stability over the studied period, which may oppose and prevent the heterogenous topical application of the CO on the skin since there is an intrinsic risk of this treatment related to the instability of the extemporaneous preparation as well as may increase the health safety of the patients. These concerns were mentioned for other pharmaceutical preparations in which there is no regulation to testify along with high-risk in quality and safety requiring proper management [34]. As reached a high value of payload of the CO into the LC system, these issues may be contoured bringing better physicochemical characteristics and, simultaneously, sustaining the release of the CO into the skin layers, what is possible for this LC system due the colloidal and chemical stabilities [12].

The chromatographic analyses allowed to identify phorbol esters in the CO matrix. These compounds exhibit unusual structural characteristics that undergo neutral loss of mono- or diesters through different fragmentation mechanisms, yielding the ion m/z 311 related to the basic phorbol skeleton, and the transition m/z 311 \rightarrow 293, which is typically associated with the loss of a water molecule due to the presence of hydroxyl groups in the phorbol structure [35]. An example that confirms this, is the mass feature m/z 539.26 (retention

time = 5.65) could potentially correspond to a compound previously characterized from the leaves of *Croton tiglium* [4]. The fragmentation observed in this study correlates to the one proposed for *Euphorbia umbellata* latex dichloromethane fraction [36], another species of Euphorbiaceae family.

The higher cytotoxicity observed for the fractions, when compared with the oil matrix, can be attributed to the fractionation process, which concentrates the compounds and increases their cytotoxic effects [16]. On the other side, the formulation 8A presented cytotoxicity at lower concentrations, primarily due to the presence of the surfactant (polyethylene glycol hexadecyl ether). It is known that surfactants can be toxic to cultured cells, disrupting the integrity of the cytoplasmic membrane [37]. In fact, these surfactants, which possess detergent properties, have been used for cellular permeabilization and have shown efficacy in the induction of cell death [38-39]. However, it is important to consider that direct contact of the LC formulation with the skin may lead to intense and persistent inflammatory reactions. Therefore, additional skin tests should be conducted to evaluate whether the formulation causes any damage or leaching of harmful substances to the skin tissue.

CONCLUSION

The study evaluated different formulations for the development of a liquid crystal system as a vehicle for deep chemical peel preparations, using croton oil as oily phase, water as an aqueous phase and a surfactant (polyethylene glycol hexadecyl ether). Among the formulations tested, the one composed of 10% polyethylene glycol hexadecyl ether, 10% croton oil, and 80% aqueous phase (w/w/w) showed promising physical characteristics. To further enhance its properties, hydroxyethyl cellulose (0.5%, w/w) was added. The liquid crystal system successfully loaded the croton oil, with the phorbol esters identified in the vegetable matrix. The LC system demonstrated stability over a 28-day period in a stability study. The cytotoxic study demonstrated that the vegetal matrix (croton oil) presented low cytotoxicity against the cell model studied. However, the fractionation process increased the concentration of terpenes (diterpenes), which correlated with an increase in cytotoxicity. The developed formulation also demonstrated cytotoxicity, but this effect could be attributed to the surfactant's action over the cells. Further *in vivo* studies are suggested to assess the formulation's effects. Nonetheless, the formulation shows promising potential as a carrier for croton oil in deep chemical peel procedures.

Funding: "This research was funded by Conselho Nacional de Desenvolvimento Científico e Tecnológico - CNPq, grant number 407347/2021-6, Chamada CNPq/MCTI/FNDCT N° 18/2021 - Faixa A - Grupos Emergentes".

Acknowledgments: The authors are grateful to CNPq for financial support and technical support of "Central de Laboratórios Multi-usuários" (CLABMU – State University of Ponta Grossa - UEPG).

Conflicts of Interest: "The authors declare no conflict of interest".

REFERENCES

1. Lee KC, Wambier CG, Soon SL, Sterling JB, Landau M, Rullan P, et al. Basic chemical peeling: Superficial and medium-depth peels. *J Am Acad Dermatol*. 2019 Aug;81(2):313–24.
2. Hetter GP. An examination of the phenol croton oil peel: Part IV. Face peel results with different concentrations of phenol and croton oil. *Plast Reconstr Surg*. 2000 Mar;105(3):1061–83.
3. Wambier CG, Lin E, Roderjan A, Beltrame FL, Döll-Boscardin PM, Celidonio TC, et al. Updates on level of evidence of clinical efficacy of facial phenol-croton oil peels and comments on history and mechanisms of action. *Int J Dermatol*. 2022 Nov;62(7):1-3.
4. Zhang DD, Zhou B, Yu JH, Xu CH, Ding J, Zhang H, et al. Cytotoxic tigliane-type diterpenoids from *Croton tiglium*. *Tetrahedron*. 2015 Dec;71(52):9638–44.
5. Kim MS, Kim HR, So HS, Lee YR, Moon HC, Ryu DG, et al. Crotonis fructus and its constituent, croton oil, stimulate lipolysis in OP9 adipocytes. *Evid Based Complement Alternat Med*. 2014 Jan; 2014:1–5.
6. Justo AS, Lemes BM, Nunes B, Antunes KA, Capote ACMO, Lipinski LC, et al. Characterization of the activity of *Croton tiglium* oil in Hetter's very heavy phenol–croton oil chemical peels. *Dermatol Surg*. 2021 Mar;47(7):944-6.
7. Andrade FF, Santos ODH, Oliveira WP, FILHO PAR. Influence of PEG-12 Dimethicone addition on stability and formation of emulsions containing liquid crystal. *Int. J. Cosmet. Sci*. 2007 Jan; 29:211-18.
8. D'Errico G, Ciccarelli D, Ortona O. Effect of glycerol on micelle formation by ionic and nonionic surfactants at 25 degrees. *C. J Colloid Interface Sci*. 2005 Jun;286(2):747–54.
9. Liu P, Gao W, Zhang Q, Chen K, Zhang J, Chen L, et al. Temperature-sensitive hydrogel modified by polymerizable liquid crystal AAC-Brij-58: Optical and protein adsorption/desorption behaviors. *React Funct Polym*. 2015 Apr;89:1–8.
10. Tan LCR, Hamdan S, Doreen SHN. Association behavior of polyoxyethylene (20) cetyl ether (Brij 58) and polyoxyethylene (20) sorbitan monooleate (Tween 80) with polyoxyethylene (4) lauryl ether (Brij 30). *J Sci Technol UTHM*. 2009 Dec;1-12.

11. Oyafuso MH, Carvalho FC, Takeshita TM, Luiza A, Ribeiro D, Merino V, et al. Development and *in vitro* evaluation of lyotropic liquid crystals for the controlled release of dexamethasone. *Polymer*. 2017 Aug;9(8):330–46.
12. Campos M, Garcia S, Mussi SV, Figueiredo SA, Carvalho M, José M, et al. Liquid crystalline nanodispersion functionalized with cell-penetrating peptides improves skin penetration and anti-inflammatory effect of lipoic acid after *in vivo* skin exposure to UVB radiation. *Drug Deliv Transl Res*. 2020 Aug;10(6):1810–28.
13. Chountoulesi M, Pispas S, Tseti IK, Demetzos C. Lyotropic liquid crystalline nanostructures as drug delivery systems and vaccine platforms. *Pharmaceuticals*. 2022 Apr;15(4):429.
14. Silvestrini AVP, Debiasi BW, Praça FG, Bentley MVLB. Progress and challenges of lyotropic liquid crystalline nanoparticles for innovative therapies. *Int J Pharm*. 2022 Nov;628:122299.
15. Fan JP, He CH. Simultaneous quantification of three major bioactive triterpene acids in the leaves of *Diospyros kaki* by high-performance liquid chromatography method. *J Pharm Biomed*. 2006 Jun;41(3):950–6.
16. Cruz LS, Kanunfre CC, Andrade EA, Oliveira AA, Cruz LS, Moss MF, et al. enriched terpenes fractions of the latex of *Euphorbia umbellata* promote apoptosis in leukemic cells. *Chem Biodivers*. 2020 Sep;17: e2000369.
17. Terescenco D, Picard C, Clemenceau F, Grisel M, Savary G. Influence of the emollient structure on the properties of cosmetic emulsion containing lamellar liquid crystals. *Colloids Surf*. 2018 Jan;536:10–9.
18. Nunes KM, Teixeira CCC, Kaminski RCK, Sarmento VHV, Couto RO, Pulcinelli SH, et al. The monoglyceride content affects the self-assembly behavior, rheological properties, syringeability, and mucoadhesion of in situ-gelling liquid crystalline phase. *J Pharm Sci*. 2016 Aug;105(8):2355–64.
19. Castro, RML. [Emulsion: A literature review [dissertation]]. João Pessoa (PB): Universidade Federal da Paraíba; 2014.
20. Silva PB, Calixto GMF, Júnior JAO, Bombardelli RLA, Fonseca-Santos B, Rodero CF, et al. Structural features and the anti-inflammatory effect of green tea extract-loaded liquid crystalline systems intended for skin delivery. *Polymer*. 2017 Jan;9(12):30.
21. Milak S, Zimmer A. Glycerol monooleate liquid crystalline phases used in drug delivery systems. *Int J Pharm*. 2015 Jan;478(2):569–87.
22. Hyde, Stephen. Identification of lyotropic liquid crystalline mesophases. *Handbook of Applied Surface and Colloid Chemistry*. John Wiley & Sons, Ltd. New York, NY, USA: 2001. p. 299–332.
23. Amar-Yuli, I, Garti N. Transitions induced by solubilized fat into reverse hexagonal mesophases. *Colloids Surf B*. 2005 Jun;43(2):72–82.
24. Santos ODH, Sacai F, Ferrari M, Rocha Filho PA da. Liquid crystals in O/W emulsions with urea: development and testing. *Cosmetics & toiletries*. 2004; 119(12):83-8.
25. Hong-in P, Chaiyana W. Potential cosmeceutical lamellar liquid crystals containing black longan (*Dimocarpus longan* Lour.) seed extract for MMP-1 and hyaluronidase inhibition. *Sci Rep*. 2022 May;12(1):7683.
26. Velasco MVR, Okubo FR, Ribeiro ME, Steiner D, Bedin V. Rejuvenescimento da pele por *peeling* químico: enfoque no *peeling* de fenol. *An. Bras. Dermatol*. 2004 Feb;79(1):91–9.
27. Nekkanti V, Karatgi P, Prabhu R, Pillai R. Solid self-microemulsifying formulation for candesartan cilexetil. *AAPS Pharm Sci Tech*. 2009 Dec 15;11(1):9–17.
28. Hunter TN, Pugh RJ, Franks GV, Jameson GJ. The role of particles in stabilising foams and emulsions. *Adv Colloid Interface Sci*. 2008 Mar;137(2):57–81.
29. Wambier CG, Lee KC, Soon SL, Sterling JB, Rullan PP, Landau M, et al. Advanced chemical peels: Phenol-croton oil peel. *J Am Acad Dermatol*. 2019 Aug;81(2): 327-336.
30. Neitzke IC, Curi DG, Lin EM, Kachiu CL, Soon SL, Bittencourt ACL, et al. Translational research on the role of formula stability in Hetter's phenol-croton oil peels: Analysis of chemical studies and clinical outcomes from a randomized, double-blinded, split-face controlled trial. *J Am Acad Dermatol*. 2021 Mar;84(3):854-6.
31. Chong JYT, Mulet X, Waddington LJ, Boyd BJ, Drummond CJ. Steric stabilisation of self-assembled cubic lyotropic liquid crystalline nanoparticles: high throughput evaluation of triblock polyethylene oxide-polypropylene oxide-polyethylene oxide copolymers. *Soft Matter*. 2011;7(10):4768-77
32. Chountoulesi M, Perinelli DR, Forys A, Bonacucina G, Trzebicka B, Pispas S, et al. Liquid crystalline nanoparticles for drug delivery: The role of gradient and block copolymers on the morphology, internal organisation and release profile. *Eur J Pharm Biopharm*. 2021 Jan;158:21–34.
33. Rodero CF, Calixto GMF, Santos KC, Sato MR, Ramos AS, Miró MS, et al. Curcumin-loaded liquid crystalline systems for controlled drug release and improved treatment of vulvovaginal candidiasis. *Mol Pharmaceutics*. 2018 Sep;15(10):4491–504.
34. Kiseļova O, Mauriņa B, Šidlovska V, Zvejnieks J. The extent of extemporaneous preparation and regulatory framework of extemporaneous compounding in Latvia medicina. 2019 Aug 26; 55(9):531.
35. Vogg G, Achatz S, A. Kettrup, Sandermann HJ. Fast, sensitive and selective liquid chromatographic-tandem mass spectrometric determination of tumor-promoting diterpene esters. *J Chromatogr A*. 1999 Sep;855(2):563–73.
36. Andrade EA, Crus LS, Machinski I, Ventura ACT, Carletto B, Paludo K, et al. Terpenes of *Euphorbia umbellata* latex are involved in cytotoxic effects against melanoma cells. *World J Pharm Pharm Sci*. 2021 April;10(4):26-37.
37. Cornelis M, Dupont C, Wepierre J. *In vitro* cytotoxicity tests on cultured human skin fibroblasts to predict the irritation potential of surfactants. *Altern Lab Anim*. 1991 July;19(3):324-36.

38. Isaksson L, Enberg J, Neutze R, Göran Karlsson B, Pedersen A. Expression screening of membrane proteins with cell-free protein synthesis. *Protein Expr Purif.* 2012 Mar;82(1):218–25.
39. Radeva G, Perabo J, Sharom FJ. P-Glycoprotein is localized in intermediate-density membrane microdomains distinct from classical lipid rafts and caveolar domains. *FEBS J.* 2005 Sep;272(19):4924–37.



© 2023 by the authors. Submitted for possible open access publication under the terms and conditions of the Creative Commons Attribution (CC BY NC) license (<https://creativecommons.org/licenses/by-nc/4.0/>).